Molecular dynamics simulation of dynamical properties of InSb

S. C. Costa,* P. S. Pizani, and J. P. Rino
Departamento de Física, Universidade Federal de São Carlos, Caixa Postal 676, 13565-905, São Carlos, SP, Brazil
(Received 31 January 2003; revised manuscript received 29 April 2003; published 28 August 2003)

Molecular dynamics simulation was used to study dynamical properties of InSb. The effective potential takes into account two and three body interactions, considering atomic size effects and charge-charge, charge-dipole, and dipole-dipole interactions between 1000 particles, 500 In and 500 Sb, initially within a cubic box of side $L=32.397$ Å. The effect of hydrostatic pressure and temperature on the dynamical properties as vibrational density of states, phonon anharmonicity, dynamic Debye-Waller factor, thermal expansion coefficient, and structural phase transformations are correctly described, in excellent agreement with the experimental results.

DOI: 10.1103/PhysRevB.68.073204 PACS number(s): 61.20.Ja, 61.43.Bn, 61.43.Dq, 62.50.+p

I. INTRODUCTION

The construction of the correct interaction potential to simulate material properties is the core of any molecular dynamics (MD) simulation. In general, a certain interaction potential which is adequate to describe some limited number of material properties may fail to describe other properties. This assertion can be considered as a general rule (with exceptions, of course) of certain interaction potentials that describe very well the static structural properties but present problems to describe dynamical properties, and vice versa.[1–3] The goal is then to construct an interaction potential able to describe the most possible properties of a given system. Once the potential is capable to describe correctly known properties of a certain material, it can be used to simulate and preview new properties, in situations very difficult to be reached or not yet discernable experimentally. In the present work, the interatomic potential which is in excellent accord with the experimental static properties of InSb such as crystal symmetry, coordination number, bond angles, phase transition induced by hydrostatic pressure and bond distances was successfully used to simulate its dynamical properties. From the molecular dynamics simulation, dynamical Debye-Waller factor, thermal expansion coefficient, pressure induced phase transition, temperature, and pressure phonon anharmonicity were correctly described, the last in excellent agreement with Raman scattering experimental results.

II. MOLECULAR DYNAMICS CALCULATION

The molecular dynamics simulations were performed using the full Parrinello-Rahman ensemble.[4] The details of the interatomic potential and all parameters used in the present simulation are described in Ref. 5, in which it was explored mainly static properties and structural phase transitions induced by pressure and temperature.[5] Here attention will focus on the dynamical behavior of the ions in the crystalline phase as a function of the temperature, at normal pressure and also under high hydrostatic external pressure. From the atomic trajectory, furnished by the MD, it is possible to calculate all positional, angular and dynamical properties of the system. The velocity autocorrelation function $Z_\alpha(t)$ is defined as

$$Z_\alpha(t)=\frac{\langle v_{i\alpha}(0)v_{i\alpha}(t)\rangle}{\langle v_{i\alpha}(0)^2\rangle},$$

where $v_{i\alpha}(t)$ is the velocity of particle i of type α at time t and $\langle\rangle$ denotes an ensemble average as well as an average over all particles of type α. The vibrational density of states $G(\omega)$ is obtained from the Fourier transform of the velocity-velocity correlation function

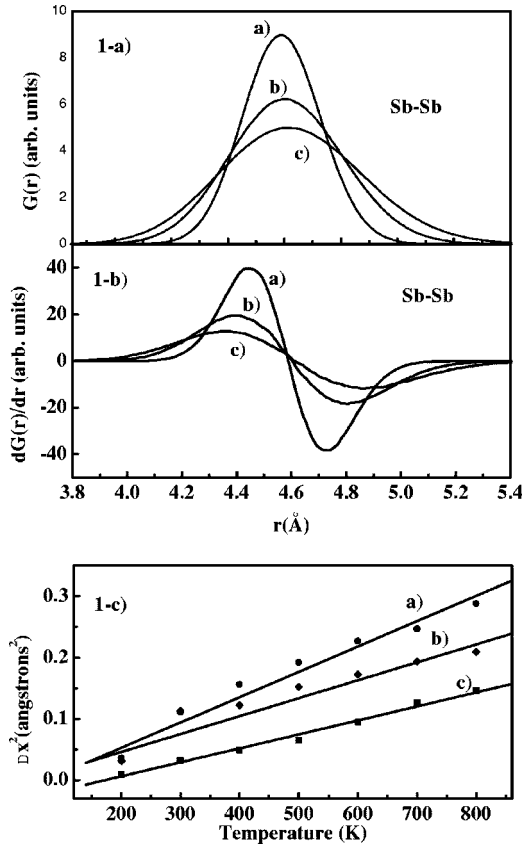

FIG. 1. (a) First peak of the pair distribution function (PDF) of Sb-Sb atoms in crystalline InSb for three different temperatures (a) 300, (b) 600, and (c) 900 K. (b) first derivative of the PDF for the three temperatures. (c) squared atomic amplitude oscillation for (a) In-In, (b) Sb-Sb, and (c) In-Sb as a function of the temperature.

TABLE I. Values of the physical constants obtained by molecular dynamics simulations and from the literature. $\alpha_{\text{Sb-Sb}}$, $\alpha_{\text{In-In}}$, $\alpha_{\text{In-Sb}}$, are the mean thermal expansion coefficient between 300 and 900 K. $(\partial\Delta x^2)/\partial T)_P$, is the temperature coefficient for the squared atomic amplitude oscillation. ω_{op} is the maximum of the optical band and $(\partial\omega_{\text{op}}/\partial T)_P$ and $(\partial\omega_{\text{op}}/\partial P)_T$ are its temperature and pressure coefficient, respectively. $(\partial\omega_{\text{LO}}/\partial T)_P$, $(\partial\omega_{\text{TO}}/\partial T)_P$, $(\partial\omega_{\text{LO}}/\partial P)_T$, $(\partial\omega_{\text{TO}}/\partial P)_T$ are the temperature and pressure frequency coefficients for the longitudinal and transverse optical phonons, respectively.

Molecular dynamics	Literature
$\alpha_{\text{Sb-Sb}}\sim 10\times10^{-6}\ \text{K}^{-1}$ $\alpha_{\text{In-In}}\sim 14\times10^{-6}\ \text{K}^{-1}$ $\alpha_{\text{In-Sb}}\sim 2\times10^{-6}\ \text{K}^{-1}$	$\alpha\sim 6\times10^{-6}\ \text{K}^{-1}$ (Ref. 14)
$\left(\frac{\partial\Delta x^2}{\partial T}\right)_P$ Sb-Sb: $2.9\times10^{-4}\ \text{Å}^2\,\text{K}^{-1}$ In-In: $4.1\times10^{-4}\ \text{Å}^2\,\text{K}^{-1}$ In-Sb: $2.3\times10^{-4}\ \text{Å}^2\,\text{K}^{-1}$	
$\omega_{\text{op}}\sim 170\ \text{cm}^{-1}$	$\omega_{\text{op}}\sim 175\ \text{cm}^{-1}$ (Ref. 10) $\omega_{\text{LO}}\sim 190.7\ \text{cm}^{-1}$ (Ref. 13) $\omega_{\text{TO}}\sim 179.7\ \text{cm}^{-1}$ (Ref. 13)
$\left(\frac{\partial\omega_{\text{op}}}{\partial T}\right)_P\sim -0.025\ \text{cm}^{-1}\,\text{K}^{-1}$	$\left(\frac{\partial\omega_{\text{LO}}}{\partial T}\right)_P\sim -0.026\ \text{cm}^{-1}\,\text{K}^{-1}$ (Ref.12) $\left(\frac{\partial\omega_{\text{TO}}}{\partial T}\right)_P\sim -0.016\ \text{cm}^{-1}\,\text{K}^{-1}$ (Ref.12)
$\left(\frac{\partial\omega_{\text{op}}}{\partial P}\right)_T\sim 10\ \text{cm}^{-1}\,\text{GPa}^{-1}$	$\left(\frac{\partial\omega_{\text{LO}}}{\partial P}\right)_T\sim 4.2\ \text{cm}^{-1}\,\text{GPa}^{-1}$ (Ref.13) $\left(\frac{\partial\omega_{\text{TO}}}{\partial P}\right)_T\sim 4.7\ \text{cm}^{-1}\,\text{GPa}^{-1}$ (Ref.13)

$$G_\alpha(\omega)=\frac{6N_\alpha}{\pi}\int_0^\infty Z_\alpha(t)\cos(\omega t)dt.$$

From the temperature dependence of the pair distribution function (PDF), which gives the bond distance between pair of atoms, the dynamical Debye-Waller factor and the thermal expansion coefficient can be obtained.

III. RESULTS AND DISCUSSION

Among the several static structural information that can be obtained from the pair distribution function (PDF) as bond length, atomic bond angle distributions, crystalline symmetry, and coordination numbers, in variation with the temperature and pressure gives information about structural phase transitions. Moreover, the variation with the temperature furnish directly the thermal expansion coefficient while the width of the pair distribution function gives the atomic oscillation amplitude, which permits to calculate the dynamical Debye-Waller factor. The data were obtained from the simulation in steps of 50 K, from 200 to 1100 K. In Fig. 1(a) it shows the evolution of the first peak of the PDF of Sb-Sb distance for three temperatures 300, 600, and 900 K, at 0 GPa, whose maximum peak position gives the Sb-Sb bond distance. From the zeros of the derivative of the first peak, displayed in Fig. 1(b), was obtained the thermal expansion coefficient for Sb-Sb, and similarly for In-In and InSb distances. The average values between 300 and 900 K are $\alpha_{\text{Sb-Sb}}\sim 10\times10^{-6}$, $\alpha_{\text{In-In}}\sim 14\times10^{-6}$ and $\alpha_{\text{In-Sb}}\sim 2\times10^{-6}\ \text{K}^{-1}$ for the cubic phase (at 0 GPa).

From the full width of the PDF was obtained the atomic oscillation amplitude for In-Sb, In-In, and Sb-Sb atoms Δx as a function of the temperature, as displayed in Fig. 1(c). From a linear fit approximation, the temperature coefficient for Δx^2, $(\partial\Delta x^2)/\partial T)_P$, was obtained. The values are displayed in Table I. From these values, it can be determined the dynamical Debye-Waller factor by using the equation[6]

$$D(T)=\exp[-2M(T)]=\exp\left[\frac{-4\pi^2(\Delta x)^2}{3d^2}\right],$$

where d is the reticular spacing for the planes giving rise to the reflection under consideration.

Figure 2 displays the vibrational density of states $G(\omega)$ simulated at 0 GPa and 300 K, obtained by the Fourier transforms of the velocity-velocity correlation function and in comparison with the results obtained by the deformable bond model (DBM),[7] the experimental Raman spectrum[8] and with the phonon dispersion curve.[9] The result from MD fits very well the DBM and experimental results, reproducing the correct frequencies of the acoustical and optical bands. The lower values of the frequencies obtained from MD simulations can be attributed to the small number of particles (1000), since it sampled only around 80% of the high values

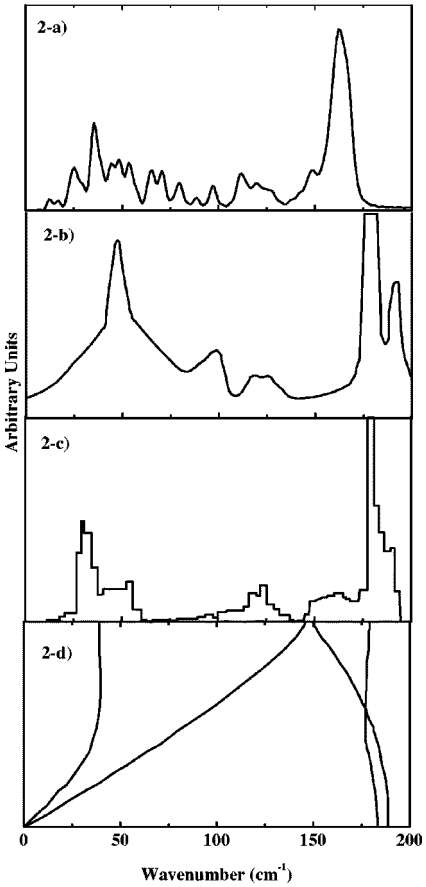

FIG. 2. (a) Vibrational density of states $G(\omega)$ from the molecular dynamics simulation at 0 GPa and 300 K. (b) Raman spectrum of InSb, Ref. 8. $G(w)$ from the deformable bond model, Ref. 7. (c) $G(w)$ from the deformable bond model, Ref. 7. (d) phonon dispersion curve for InSb, Ref. 9.

of the wave vector side of the Brillouin zone, while Raman scattering samples phonons at the center of the Brillouin zone (phonon wave vectors $k\sim 0$). As the dispersion relation of the optical modes presents decreasing frequencies with increasing phonon wave vectors, it is expected then lower values of the phonon frequencies from the simulations. Furthermore, the Raman scattering measurements from Ref. 8 were performed at low temperature (80 K), which shifts the frequencies to higher values, standing out the differences. Despite the computational limitation, the frequency value of the maximum of the optical band is 170 cm^{-1}, near 175 cm^{-1}, the average frequency value of the optical band of InSb, at room temperature.[10] A discussion on the average optical frequency ω_{op} can be found in literature, which is defined by

$$\omega_{op}=\frac{1}{3N}\sum_{k,,j}\omega_j(k),$$

where k belongs to the first Brillouin zone and j are the optical branches. This equation describes the lattice dynamics as an Einstein approximation, where the optical modes are represented by $3N$ oscillators vibrating at the same frequency ω_{op}.[11]

Figure 3(a) shows the effect of the temperature variation

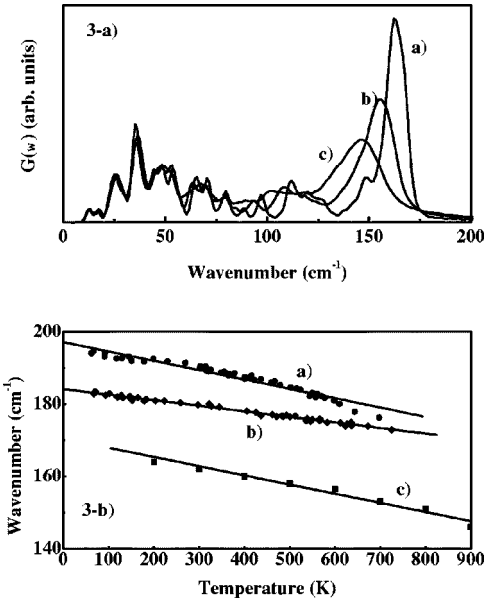

FIG. 3. (a) Vibrational density of states $G(\omega)$ at 300, 600, and 900 K. (b) (a) and (b) temperature dependence of the longitudinal and transverse optical phonon frequencies from Raman scattering, respectively and (c) temperature dependence of the maximum of $G(\omega)$ in the optical range obtained by molecular dynamics simulation. The full lines are linear fitting approximations.

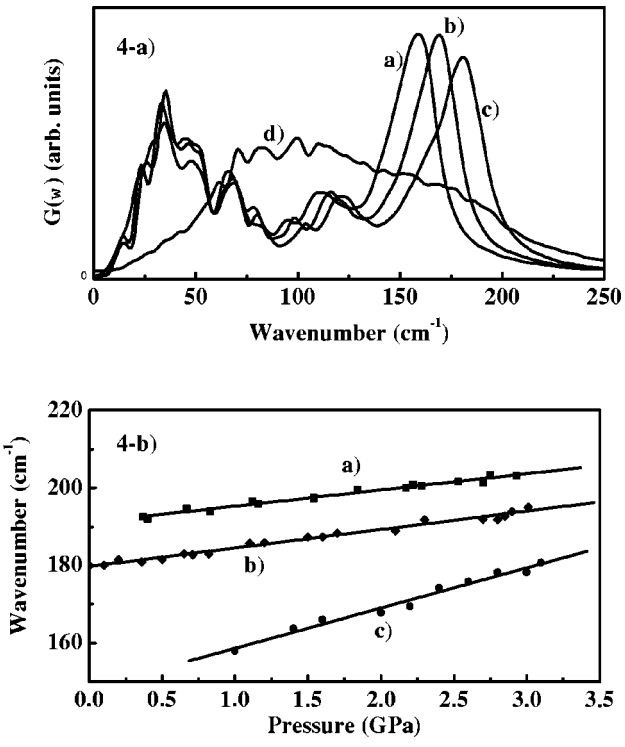

FIG. 4. (a) Pressure dependence of $G(\omega)$, from molecular dynamics simulation at (a) 1.0 GPa, (b) 2.0 GPa, (c) 3.0 GPa, and (d) 3.2 GPa. (b) (a) and (b) pressure dependence of the longitudinal and transverse optical phonon frequencies from Raman scattering, respectively, from Ref. 12 and (c) pressure dependence of the maximum of $G(\omega)$ in the optical range obtained by molecular dynamics simulation. The full lines are linear fitting approximations.

on $G(\omega)$, for 300, 600, and 900 K. The simulations were performed from 200 to 1100 K, in steps of 50 K. Figure 3(b) displays the temperature dependence of the longitudinal (LO) and transverse (TO) optical phonon frequencies of InSb obtained by Raman scattering experiment[12] and the maximum of the optical band of the density of states, from the MD simulation. From a linear fitting approximation, the temperature frequency coefficients $(\partial\omega_{\mathrm{LO}}/\partial T)_P$, $(\partial\omega_{\mathrm{TO}}/\partial T)_P$, and $(\partial\omega_{\mathrm{op}}/\partial T)_P$ are $^{-}0.026$, -0.016, and -0.025 $\mathrm{cm}^{-1}\,\mathrm{K}^{-1}$, respectively.

Figure 4(a) shows the dependence of the $G(\omega)$ with the hydrostatic pressure. There are two main effects of the pressure on $G(\omega)$: (i) an anharmonic frequency shift to high frequencies up to 3.0 GPa and (ii) a structural cubic to orthorhombic phase transition, denounced by the dramatic change in $G(\omega)$ at about 3.2 GPa. Figure 4(b) displays the pressure dependence of the longitudinal optical phonon of crystalline InSb from Raman scattering[13] and of the maximum of $G(\omega)$. From a linear fitting approximation, the pressure frequency coefficients $(\partial\omega_{\mathrm{LO}}/\partial P)_T$, $(\partial\omega_{\mathrm{TO}}/\partial P)_T$, and $(\partial\omega_{\mathrm{op}}/\partial P)_T$ are 4.2, 4.7, and 10 $\mathrm{cm}^{-1}\,\mathrm{GPa}^{-1}$, respectively. Finally, Table I summarizes all numerical values obtained from the present simulation, showing also the experimental values discernable in the literature.

IV. CONCLUSIONS

Summarizing, isoenthalpic-isobaric molecular dynamics simulations to study the pressure and temperature influence on dynamical properties of InSb was successfully performed using the effective potential which takes into account two and three body interactions. From the pair distribution function, the thermal expansion coefficient was obtained, in excellent accord with the experimental value. Furthermore, the temperature dependence of the dynamical Debye-Waller factor was also obtained. From the vibrational density of states, the temperature and pressure phonon anharmonicity was correctly described, in excellent accord with results from Raman scattering. As the interatomic potential describes very well static and dynamic properties of InSb, it can be used to simulate and preview new properties in several different experimental conditions.

ACKNOWLEDGMENTS

This work was partially supported by Fundação de Amparo à Pesquisa do Estado de São Paulo–FAPESP and Conselho Nacional de Desenvolvimento Científico e Tecnológico–CNPq.

*Electronic address: sancosta@df.ufscar.br

[1] M.A.P. Silva, A. Monteil, Y. Massaddeq, and S.J.L. Ribeiro, J. Chem. Phys. **117**, 5366 (2002).

[2] S. Hayakawa, A. Osaka, H. Nishioka, S. Matsumoto, and Y. Miura, J. Non-Cryst. Solids **272**, 103 (2000).

[3] K. Vollmayer, W. Knob, and K. Bindder, Phys. Rev. B **54**, 15 808 (1996).

[4] M. Parrinello and A. Rahman, Phys. Rev. Lett. **45**, 1196 (1980); M. Parrinello and A. Rahman, J. Appl. Phys. **52**, 7182 (1981).

[5] S.C. Costa, P.S. Pizani, and J.P. Rino, Phys. Rev. B **66**, 214111 (2002).

[6] A. Guinier, *X-Ray Diffraction in Crystals, Imperfect Crystals and Amorphous Bodies* (W.H. Freeman and Company, San Francisco, 1963), Chap. 7.

[7] K. Kunc, M. Balkanski, and M.A. Nusimovici, Phys. Status Solidi B **72**, 229 (1975).

[8] W. Kiefer, W. Richter, and M. Cardona, Phys. Rev. B **12**, 2346 (1975).

[9] D.L. Price, J.M. Rowe, and R.M. Nicklow, Phys. Rev. B **3**, 1268 (1971).

[10] G. Landa, Ph.D. thesis, Université Paul Sabatier, Toulouse, France, 1990.

[11] R. Carles, G. Landa, and J.B. Renucci, Solid State Commun. **53**, 179 (1985).

[12] E. Liarokapis and E. Anastassakis, Phys. Rev. B **30**, 2270 (1984).

[13] K. Aoki, E. Anastassakis, and M. Cardona, Phys. Rev. B **30**, 681 (1984).

[14] *Numerical Data and Functional Relationships in Science and Technology*, edited by O. Madelung, M. Schulz, and H. Weiss, Landolt-Börnstein, New Series, Group III, Vol. 17a, Pt. 327 (Springer-Verlag, Berlin, 1982).